Project title:	Combined thermal and visual image analysis for crop scanning and crop disease monitoring
Project number:	CP 060a
Project leader:	Dr. Nasir Rajpoot
Report:	Annual Report, March 2013
Previous report:	Annual Report, June 2012
Key staff:	Shan-e-Ahmed Raza Dr. Nasir Rajpoot Dr. John Clarkson
Location of project:	University of Warwick
Industry Representative:	Alan Davis
Date project commenced:	11 March 2011
Date project completed (or expected completion date):	10 March 2014

DISCLAIMER

AHDB, operating through its HDC division seeks to ensure that the information contained within this document is accurate at the time of printing. No warranty is given in respect thereof and, to the maximum extent permitted by law the Agriculture and Horticulture Development Board accepts no liability for loss, damage or injury howsoever caused (including that caused by negligence) or suffered directly or indirectly in relation to information and opinions contained in or omitted from this document.

AUTHENTICATION

We declare that this work was done under our supervision according to the procedures described herein and that the report represents a true and accurate record of the results obtained.

Dr. Nasir Rajpoot
Associate Professor
University of Warwick

Signature ..... Date .....

Dr. John Clarkson
Principal Research Fellow
University of Warwick

Signature ..... Date .....

Report authorised by:

[Name]
[Position]
[Organisation]

Signature ..... Date .....

[Name]
[Position]
[Organisation]

Signature ..... Date .....

CONTENTS

GROWER SUMMARY 1
Headline 1
Background 1
Summary 1
Financial Benefits 3
Action Points 3
SCIENCE SECTION 4
Introduction 4
Materials and methods 6
Experiments and Results 17
Conclusions and Future Work 22
References 23

GROWER SUMMARY

Headline

Thermal images combined with visible light images have successfully identified stressed regions of a plant canopy with high accuracy.

Background

Thermal imaging has been shown to be suitable for stress and early disease detection in plants. However, there are problems associated with thermal imaging because of variation in the perceived temperature caused by various environmental factors. These include structure of the canopy, sunlit and shaded regions, leaf angles and the distance of imaging device from the plant. The major aim of the project is to combine information from colour and thermal images to model these variations as a function of leaf angles, light intensity and 3D depth information. Results to date have shown that, with the help of statistical parameters and classification algorithms, water stressed and well watered canopies can be successfully distinguished. . Thermal and stereo colour images have been collected from powdery mildew inoculated tomato plants and these are now being processed. This will include developing algorithms for accurate alignment of the thermal and colour images to create a depth map of the plant for analysis. The aim is to develop a 3D thermal profile of a crop to account for noise introduced due to the structure of canopy and develop new methods for early disease detection.

Summary

1. Thermal and stereo colour images were taken for 15 consecutive days from a tomato powdery mildew trial underway at Warwick Crop Centre (courtesy of Gillian Prince). Manual measurements of leaf temperature were also taken for two days. An algorithm has been developed for image rectification which is a pre-processing step before 3-D depth estimation. The process consists of aligning the same features from stereo image pair along a set horizontal line. Before analysis the images must be aligned in such a way that the same pixel location in both the images corresponds to the same physical location on the plants. Figure 1 shows a 3D profile of a tomato plant on day1 and day14 of inoculation with powdery mildew. Corresponding thermal images overlaid on the 3D profiles are also shown. On day1, leaves look more regular in shape and they appear to be at cooler temperature than the environment at about 18-20˚C, whereas on day14 leaves are more irregular in shape and their temperature is about 21-23˚C. Algorithms for accurate alignment of

these images need to be finalised, before analysis of disease progress can be undertaken.

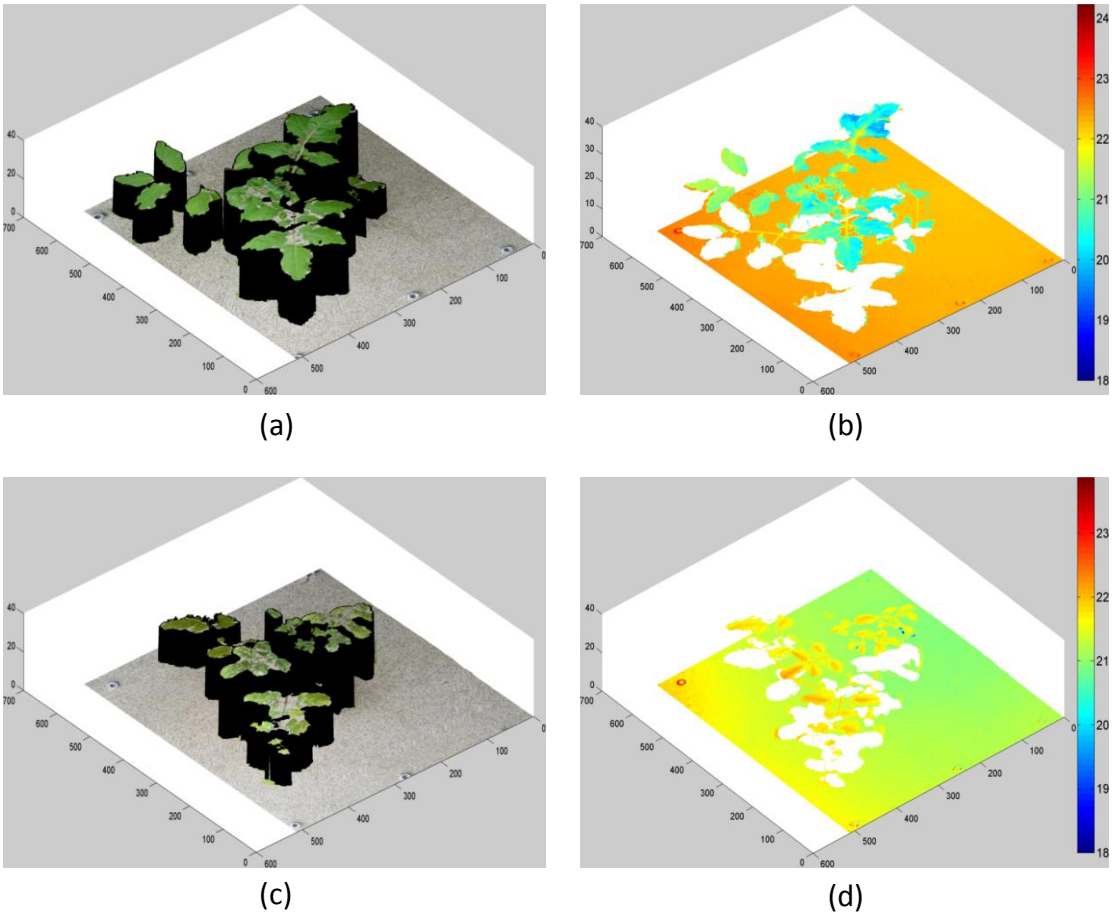

Figure 1: (a) & (c) 3D profile of a tomato plant on day1 & day14 of inoculation with powdery mildew. (b) & (d) show corresponding thermal image overlaid on 3D profile. On day1, leaves look more regular in shape and their temperature is about 18-20˚C, whereas on day14 leaves are more irregular in shape and their temperature is about 21-23˚C.

2. Thermal and colour images were obtained from a stress experiment carried out by Prof. Gail Taylor's group at the University of Southampton. 108 images of a spinach canopy were provided in total, 54 images were taken from a drought canopy and 54 images were from well-watered plants. Information from thermal and colour images was combined and machine learning techniques were used to distinguish between the two groups of plants. Results indicate that water stressed and well watered plants can be classified with an average accuracy of around 97.12%. Figure 2 shows the result of the probability of an image showing stress given by the classifier against manually measured soil moisture values for images collected from Prof. Taylor's experiment.

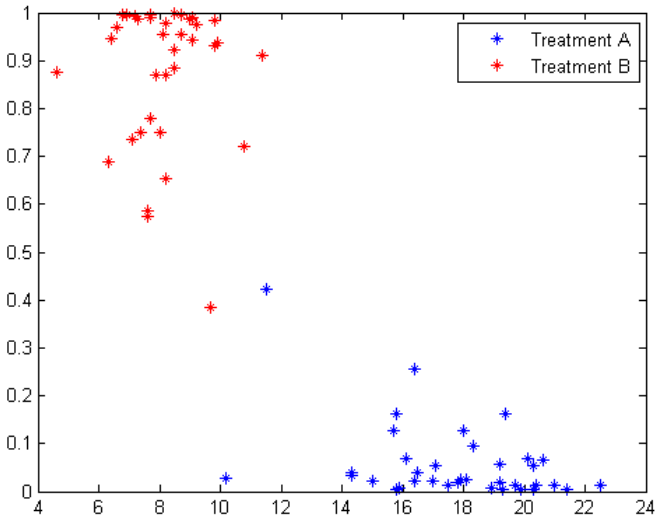

Figure 2: Probability of image showing drought-stressed plants vs soil moisture values (correlation value = - 0.89, High moisture means less probability of stress) (%Volume) as given by our classifier. Classification accuracy for this particular set of training and testing data was 98.62%.

Financial Benefits

Financial assessment is premature at this stage, although it is anticipated that stress detection in different parts of the crop could help growers to water crops more efficiently and detect disease at an early stage facilitating timely action which would mitigate against crop losses and some of the costs associated with treatment.

Action point for growers

Glasshouse growers could consider options for installing an overhead system for monitoring their crop, pending further developments as this project progresses.

SCIENCE SECTION

Introduction

Thermal imaging has been used in the past for stress and disease detection in plants [1–6]. One of the major problems associated with thermal imaging in plants is temperature variation due to canopy architecture, leaf angles, sunlit and shaded regions, environmental conditions and the distance of the plant from the camera. The major aim of this project is to combine information of stereo colour images with thermal images to overcome these problems and allow a precise 3-dimensional thermal profile of a crop to be quantified. In this report we present detail of experiments and results performed during the last year to obtain information on how we can use thermal and colour imaging for detecting disease and stress in plants, for the benefit of horticultural industry. This report contains work on images taken from two types of experiments.

1. Tomato Plants infected with powdery mildew disease performed at Warwick Crop Centre.

2. Stress experiment performed by collaborators at University of Southampton.

An experimental setup was designed and developed at the Department of Computer Science (Warwick-DCS) for simultaneous capture of stereo and thermal images of diseased/normal plants as shown in Figure 1. First the setup was tested on trial experiments at DCS and Warwick Crop Centre (WCC), for any necessary modifications. After some minor modifications the setup was used to image an experiment on tomato plants infected with powdery mildew disease at WCC supervised by Gillian Prince. Images of 72 plants were taken every day for about two weeks along with manual measurement of leaf temperatures (for two days). Currently, we are working on the pre-processing of these images prior to analysis. The pre-processing steps comprise 1) image rectification, 2) disparity estimation and 3) image registration. Image rectification is a method which is used as a pre-processing step for computing disparity (depth) [7]. The process consists of aligning the same features from stereo image pair along the same epipolar line. We have developed an algorithm for rectification of these images, which uses selective markers. We have also evaluated the performance of some disparity estimation algorithms, however, the main focus of our work is automatic registration of thermal and colour images. The aim of registration is to align thermal and colour images in such a way that the same pixel location on both images corresponds to same physical location on plant(s). Currently we are working

on developing an algorithm for automatic registration of thermal and colour image as this is the main bottle neck before the analysis of images collected from the experiment.

As part of work on stress analysis, we obtained thermal and colour images of a spinach canopy undergoing a water stress experiment from Prof. Gail Taylor's group at University of Southampton. There has been a lot of work done on stress analysis of plants using thermal imaging, however very few researchers have exploited the information from colour images for analysis. Most of the work done is by using stress indices formulated by Idso and Jackson [8], [9]. Researchers have conducted various experiments to find a relationship between different stress indices and temperature values found by thermal imaging [10], [11]. However, we have presented a new technique here to enhance the 'discriminatory power' of thermal imaging to identify parts of the canopy which are under water stress. Instead of using stress indices to identify stress regions, we combine information from colour and thermal images and use machine learning techniques to distinguish water stressed and well-watered canopies. We get information about the light intensity and green-ness of the plant from the colour images and use that information along with statistical information from thermal images to achieve this using support vector machines (SVM), Gaussian Processes Classifier (GPC) and a combination of both the classifiers. The results show that our algorithm can classify the stress regions of the canopy with an average accuracy of about 97.12%.

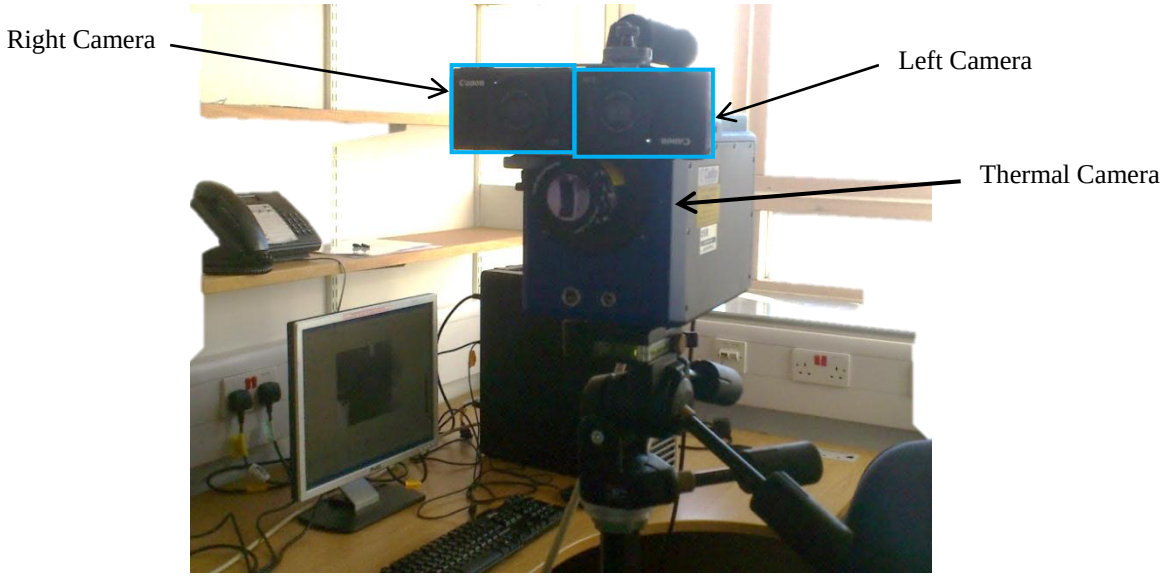

Figure 1: Front view of the camera setup

Materials and methods

Disease Detection

Development of the setup

The Cedip Titanium thermal imaging camera from the EPSRC instrument loan pool was obtained on 29th August 2012. The first step was to build and prepare a setup which can be used to capture thermal and visible light images at the same time; we also wanted to have the camera lens(s) close to each other to avoid occlusions. The setup consists of thermal imaging camera Cedip Titanium and two visible imaging cameras canon powershot S100. The visible imaging cameras were mounted on the top of the camera with the help of a support designed at Computer Science Department as shown in Figure 1. The camera setup was put to trial on plants available within Computer Science and images were taken from the setup.

Image Acquistion

The setup was ready by mid-September and moved to the WCC at Wellesbourne. A trial experiment was setup with the help of Gillian Prince which included 6 tomato plants, one uninoculated and 5 inoculated with different concentrations of the powdery mildew fungus. Images from these plants were taken for two weeks and based on the results a specific concentration of 10^6 conidia/ml was identified for future inoculation of plants with some minor modifications to the imaging process.

The experiment used for collecting the images from tomato plants consisted of 72 plants and 4 control treatments (as part of a different HDC project) and lasted for 15 days (from 04-Oct 2012 to 18-Oct-2012). The following treatments were tested for the 72 plants:

1. 18 untreated (normal) plants with no powdery mildew disease.
2. 6 plants inoculated with powdery mildew without any control treatment
3. 6 plants inoculated with powdery mildew + drench of 275.86, 7 days prior to inoculation with powdery mildew.
4. 6 plants inoculated with powdery mildew + drench of 275.86, 3 days prior to inoculation with powdery mildew.
5. 6 plants inoculated with powdery mildew + drench of 432.99, 7 days prior to inoculation with powdery mildew
6. 6 plants inoculated with powdery mildew + drench of 432.99, 3 days prior to inoculation with powdery mildew

7. 6 plants inoculated with powdery mildew + drench of 19.79, 7 days prior to inoculation with powdery mildew
8. 6 plants inoculated with powdery mildew + drench of 19.79, 3 days prior to inoculation with powdery mildew
9. 6 plants inoculated with powdery mildew + drench of 433.99, 7 days prior to inoculation with powdery mildew
10. 6 plants inoculated with powdery mildew + drench of 433.99, 3 days prior to inoculation with powdery mildew

where 275.86, 432.99, 19.79 and 433.99 are the code names for the tested products. A picture of the setup used for capturing the images is shown in Figure 2.

Figure 2: An overview of the experimental setup

Thermal and visible stereo images from these 72 plants were collected for 15 consecutive days. Manual measurements of the leaf surface temperature were also taken with the help of a temperature probe and data was collected for two days. Some of the images are shown in Figure 3

.

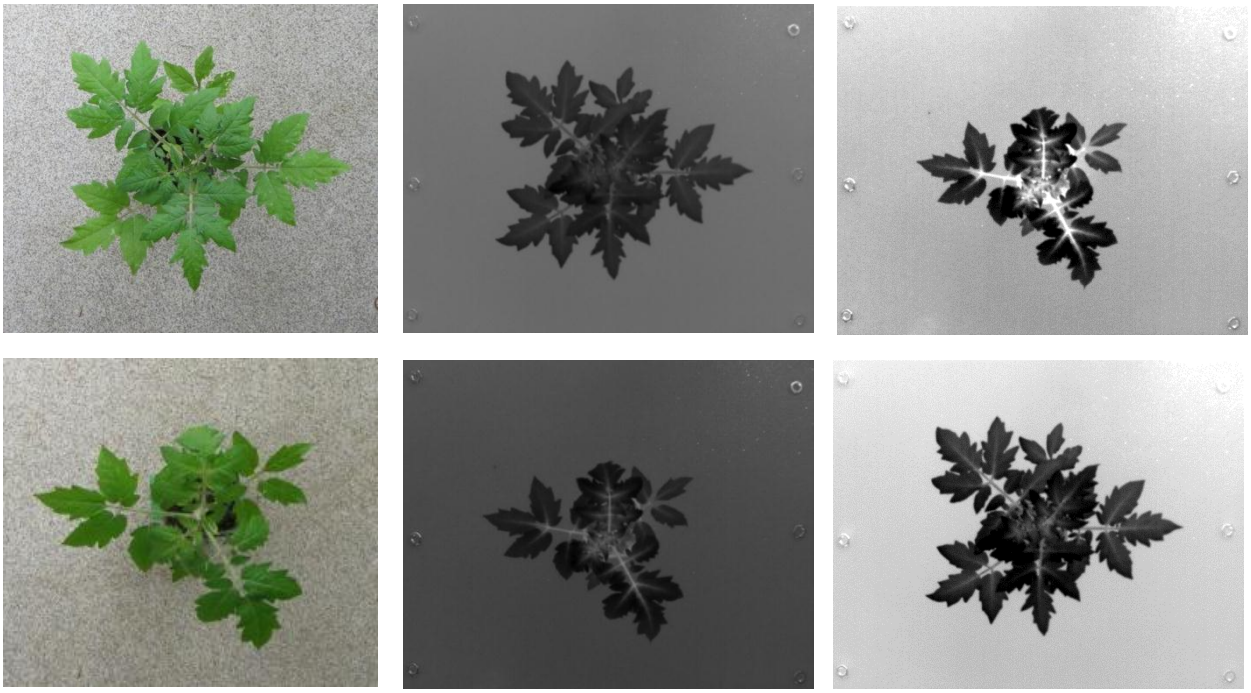

Figure 3: Sample images taken from the experiment, first two columns show raw images taken during the experiment. Third column shows enhanced thermal image for presentation purpose.

Image rectification

Image rectification is a process which consists of aligning the same features from stereo image pairs along the same epipolar line before depth estimation [12]. An example of the images is shown in Figure 4. In this figure, (a) and (b) show the images obtained from left and right cameras. In (c) both images are displayed on top of each other, the left image is displayed in red colour and the right image is shown in cyan colour and it is clear that the same features of plants do not lie on the same horizontal line. For rectification we have to align the images in such a way that we do not lose the depth information. We had placed markers at ground level for rectification purpose, as shown in Figure 4(c). By aligning the markers at the same pixel location in the images we get zero disparity at the ground level while the depth information of the plant is still retained. The algorithm used for this purpose consists of three steps.

(a) Extraction of marker points.
(b) Establishing correspondence between these points.
(c) Find the transformation

Extraction of marker points

1. Convert ‘RGB’ to ‘Lab’ colour space.
2. Perform Principal Component Analysis (PCA) on ‘a’ and ‘b’ channels.
3. Smooth the projection on 2nd principal component with Gaussian filter, sigma = 4.
4. Threshold using otsu’s method.

Establishing Correspondence between points

1. Calculate the centre of marker points.
2. Find pairwise distance between identified centres in left and right images.
3. Look for minimum distance for each identified centre in left image with the centres of right image.
4. The corresponding marker points will have minimum distance between them.
5. As a verification step, find the angle formed by joining centres in the left image with the centres in the right image. All the corresponding marker points identified in step 4 will have the same angle(s).

Find the transformation

1. Using the corresponding marker points identified in the previous step, find the transformation between the two images for rectification [13].
2. Apply the transformation on the right image to find a rectified stereo image pair.

(a) (b) (c)

Figure 4: (a) & (b) show image from left and right camera, (c) image from left camera in red and image from right camera in cyan colour.

Different steps for marker extraction are explained in Figure 5. (a) and (b) show ‘a’ and ‘b’ channels of Lab colour space for the image in Figure 4. The result of projection on 2nd principal component after performing PCA on ‘a’ and ‘b’ channels and smoothing with Gaussian is shown in (c). The result of threshold and the candidate marker points extracted

are shown in (d). The extracted marker points in the left and right image are then used in the next step to find the correspondence between the points.

Disparity estimation

Disparity is the difference in location of a point as seen by left and right cameras. The difference in location of each point in the images can be interpreted into a 3D depth map of the scene/plant under observation[14]. We have used the algorithm presented by Konolige [15] to achieve this. The algorithm for disparity estimation comprises of following steps:

1. Pre-filtering using Laplacian of Gaussian (LoG) transform to normalize image brightness and enhance texture.
2. Correspondence search along horizontal epipolar lines using a Sum of Absolute Differences (SAD) window.
3. Post-filtering with an interest operator and left/right check to eliminate bad matches.

Texture-less regions give a less reliable measure of disparity than the textured regions. The last step uses a measure of texture in a scene as an interest operator which gives high confidence to areas that are textured in intensity. We will be evaluating the results of different disparity estimation algorithms once we start the analysis.

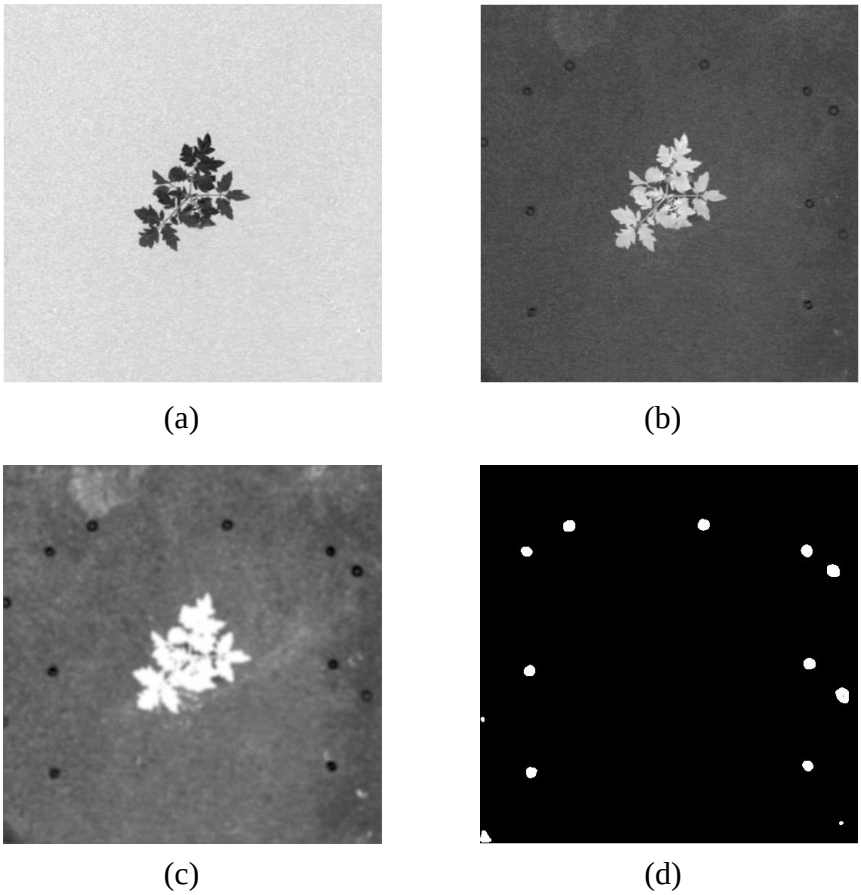

Figure 5: (a) & (b) show 'a' and 'b' channels of 'Lab' colour space for plant in Figure 4. (c) shows the result of projection on 2nd principal component after performing PCA on 'a' and 'b' channels and smoothing with Gaussian. (d) shows the result of threshold and the candidate marker points.

Thermal and colour image Registration

For combined use of thermal and colour image analysis on plants, it is necessary that the corresponding thermal and colour images are aligned in such a way that the same pixel location on both images correspond to same physical location in the plant(s). We have designed an algorithm for automatic registration of thermal and colour images in plants. The algorithm proposed for registration is as follows:

1. Convert the RGB image to Lab colour space and subtract 'a' channel from 'b' channel.
2. Remove non-uniform illumination artifacts by subtracting local mean with a window size of 55×55.
3. Denoise the results of step 2 with anisotropic diffusion filtering.
4. Calculate the gradient of colour image obtained as result of step 3 and the original thermal image using the sobel operator.
5. Perform grayscale morphological operations on both gradient images and threshold.

6. Mark the boundary points of the plants in both thermal and colour images.
7. Map the boundary obtained from colour image on the boundary obtained in thermal image.
8. Apply the same transformation in step 7, on the colour image to obtain registered colour image.

The algorithm proposed above is still under development and we are working on refining the results of our algorithm. More details about the results is presented in Experiments and Results section.

Stress Detection

Pre-processing

We obtained thermal and colour images from a stress experiment performed by Prof. Gail Taylor's group at University of Southampton. 108 images of spinach canopy were provided in total, 54 images were from a droughted canopy and 54 images were taken from well-watered plants. The images obtained from the thermal camera are shown in Figure 6. A thermal image is obtained as an image with pixel intensity values ranging from 0-255. First step is to transform the image values to temperature values. We have used a character recognition algorithm based on cross correlation which automatically recognizes the characters in the temperature bar in Figure 6(c) and identifies the temperature range for the thermal image [16]. Then we replace the image values which range from 0-255 with temperature values.

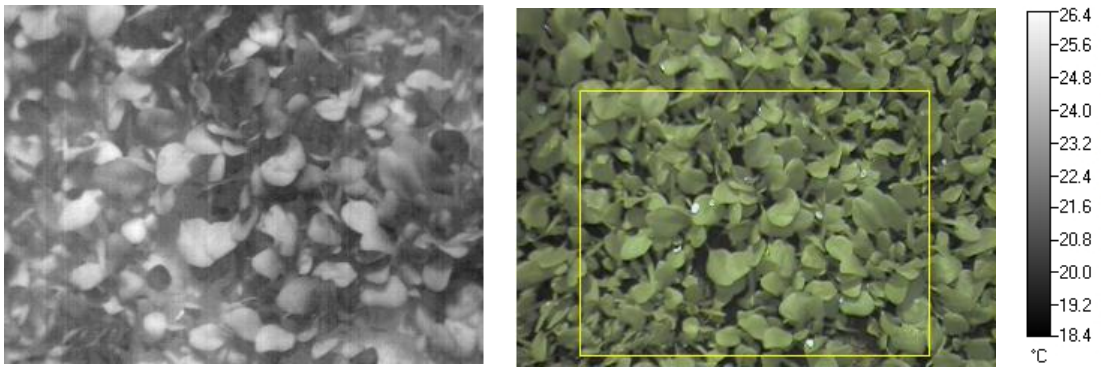

(a) (b) (c)

Figure 6: Image(s) obtained using a thermal imaging camera (NEC Thermo TracerTH9100 Pro). (a) shows thermal image with pixel values ranging from 0-255. (b)Rectangle shows region corresponding to thermal image in the colour image. (c) shows the corresponding temperature range.

To get useful information from the images, both images must be aligned so that same pixel location in both images corresponds to same physical location in the plant. Since both

thermal and colour images are coming from a single camera where there is a fixed transformation between thermal and colour images, we first find transformation between a pair of thermal and colour images by manually selecting control points and then we apply this transformation to all the images. To reduce the amount of noise present in the colour image, we apply anisotropic diffusion filtering [17]. The sample images in Figure 6 obtained after pre-processing are shown in Figure 7. The rest of the calculations are done on the pre-processed images.

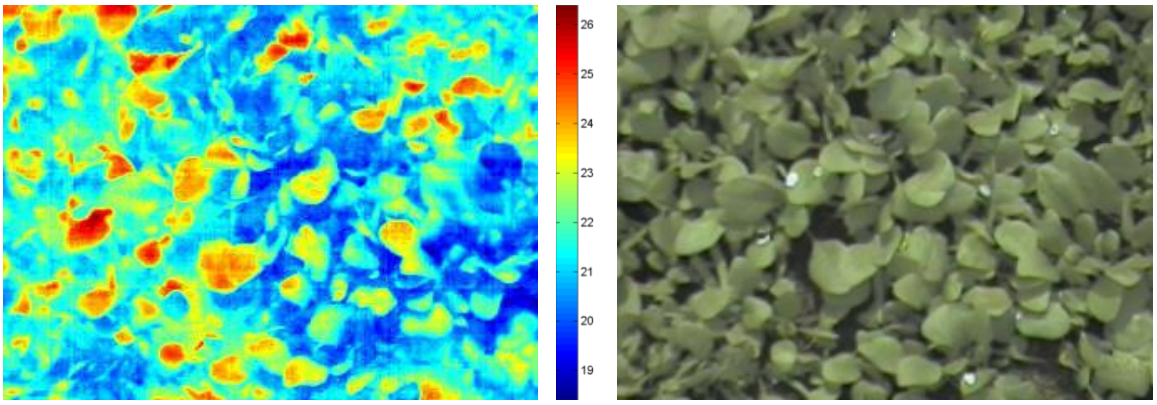

Figure 7: Colour thermal images of Figure 6 obtained after pre-processing; (a) thermal image in Figure 6(a) has been replaced by temperature values. (b) colour image in Figure 6(b) has been transformed to match thermal image in a way that same pixel locations correspond to same point located on the plant.

Feature Computation

Features were selected on the basis of observations made by various researchers [2], [18–22]. We select average values and variation in thermal profile of canopy and combine it with information from the colour image. As a first step we transformed the colour space of the colour image from RGB to Lab colour space as shown in **Error! Reference source not found.**. In Lab colour space instead of Red, Green and Blue channels, we have L-channel for luminance, 'a' and 'b' channel as the colour components. Features selected for our experiments are given in

Table **1.**

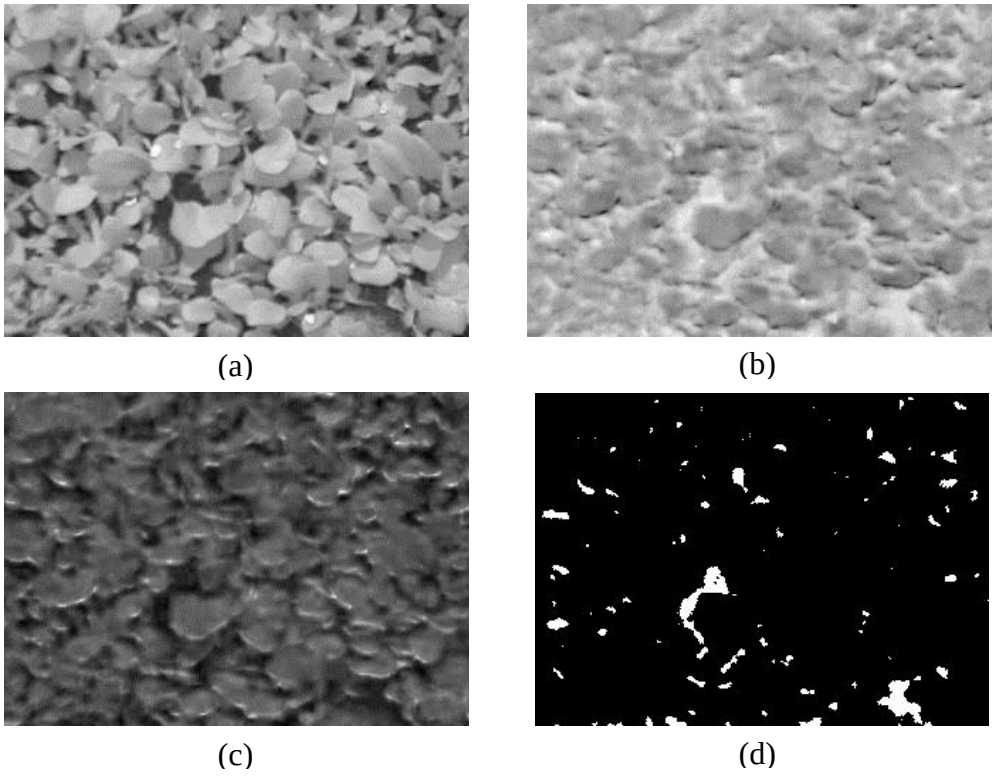

Figure 8: (a), (b) and (c) show 'L', 'a' and 'b' channels of the colour image. (d) shows the thresholded a-channel.

Table 1: Features selected for our experiments. Feature type shows that corresponding feature contains information about colour (C) or thermal (T) data or both (C/T).

	Symbol	Description	Type	p-value
1.	μ_{LT}	Luminance has been found to be a major factor to affect the thermal profile of an image [20]. In our work we scale the temperature values with the corresponding L-channel of the colour image so that the effect of light intensity is incorporated into our model. After scaling temperature data with the L-channel we take the mean of the temperature values in an image as a feature.	C/T	1.54×10^{-01}
2.	μ_a	The colour information tells us about the amount of area covered by the plants or other type of regions. In **Error! Reference source not found.**(b), lower intensities correspond to green parts of the plant whereas the background is at higher intensity value. For this reason we use the mean of the a-channel in our set of features.	C	1.92×10^{-07}
3.	μ_b	Similar to feature 2, in **Error! Reference source not found.** (c) darker regions correspond to background and so we add the mean of the b-channel to our set of	C	1.67×10^{-04}

	Symbol	Description	Type	p-value
		features.		
4.	σ_{nT}	The amount of variation present in an image is also important [2]. We normalize each row of the temperature data by its median and then take the standard deviation of the temperature values as a feature, to find the amount of variation in the canopy region covered by the image.	T	2.89×10^{-19}
5.	$\mu_{\mathit{a}\mathrm{T}}$	In Lab colour space lower values in a-channel correspond to Green region. We threshold the a-channel using Otsu's method to find the background regions as represented by white pixels in **Error! Reference source not found.** (d). We discard temperature values corresponding to background and calculate mean of temperature values corresponding to rest of pixels, as a measure of mean temperature at green parts of the plant.	C/T	1.88×10^{-21}
6.	$\sigma_{\mathit{a}\mathrm{T}}$	Similar to feature 5, we discard the temperature values corresponding to background and calculate standard deviation of temperature values corresponding to rest of pixels as a measure of variation in thermal intensities at green parts of the plant.	C/T	1.024×10^{-04}
7.	μ_{T}	Mean of temperature values	T	1.46×10^{-21}
8.	σ_{T}	Standard Deviation of temperature values	T	1.12×10^{-04}

Support Vector Machines (SVM)

Support Vector Machines (SVM) [23] is a supervised learning method used for classification and regression analysis. SVM constructs a hyperplane in high dimensional space and tries to find the hyperplane which maximizes the separation between two classes of training data points. In this work, we have used linear SVM which uses the model

$$y = \mathbf{w}^T \mathbf{x} + b \tag{1}$$

where $\mathbf{x} = [\mu_{\mathrm{LT}}, \mu_a, \mu_b, \sigma_{\mathrm{nT}}, \mu_{\mathit{a}\mathrm{T}}, \sigma_{\mathit{a}\mathrm{T}}, \mu_{\mathrm{T}}, \sigma_{\mathrm{T}}]$ denotes the input feature vector for an image and *y* denotes the classification output (+1 for plants undergoing water stress, and −1 for well-watered plants). SVM models the parameters *b* and **w** to find the maximum margin hyperplane between data points from two classes.

Gaussian Processes for Classification

Gaussian Processes can be defined as a class of probabilistic models comprising of distributions over functions instead of vectors [24–26]. A Gaussian distribution can be expressed by a mean vector and a covariance matrix. A Gaussian Process (GP) is fully characterized by its mean and covariance functions. In machine learning, GPs have been used for regression analysis and classification. Similar to SVM, Gaussian Process Classifiers (GPCs) also belong to the class of supervised classification methods. However, instead of giving discriminant function values it produces output with probabilistic interpretation, i.e. a prediction for $p(y=+1|\mathbf{x})$ which denotes the probability of assigning a label (*y*) value +1 to the input feature vector **x** [27]. GPCs do not calculate this probability directly on the input variables and assume that that the probability of belonging to a class is linked to an underlying latent function. Given a training set $D=\{(\mathbf{x}_i, y_i)|i=1,2,...n\}$ consisting of training images of both classes (water stress and well-watered) with manually assigned labels y_i to the corresponding feature vectors $\mathbf{x}_i$ extracted from those images, to make predictions about the label of the feature vectors computed from an unseen image $\mathbf{x}_*$, we have posterior probability

$$p(y_*=+1|D,\mathbf{x}_*)=\int p(y_*=+1|f_*)\,p(f_*|D,\mathbf{x}_*)df_* \tag{2}$$

The probability of belonging to a class $y_i=+1$ for an input $\mathbf{x}_i$ (known data point) is related to the value f_i of a latent function *f*. The latent function *f* is a GP which models the likelihood of one class versus the other over the *x*-axis [28]. This relationship is defined with the help of a squashing function. In our case, we use Gaussian cumulative distribution function as the squashing function.

$$p(y=+1|f_i)=\frac{1}{2}\left[1+\frac{erf\,(y_i f_i)}{\sqrt{2}}\right] \tag{3}$$

where $erf(z)$ is the error function defined as $erf(z)=\frac{2}{\sqrt{\pi}}\int_0^z e^{-t^2}dt$.The second term in the integral in equation (2) is given by,

$$p(f_*|D,\mathbf{x}_*)=\int p(f_*|\mathbf{X},\mathbf{x}_*,\boldsymbol{f})\,p(\boldsymbol{f}|D)d\boldsymbol{f} \tag{4}$$

where $\mathbf{X}=[\mathbf{x}_1,\mathbf{x}_2,...,\mathbf{x}_n]$ and $\boldsymbol{f}=[f_1, f_2,....f_n]$, *n* is the number of samples. $p(\boldsymbol{f}|D)$ can be formulated by the Bayes' rule as follows,

$$p(\boldsymbol{f} \mid D) = \frac{p(\boldsymbol{f} \mid \mathbf{X})}{p(\boldsymbol{y} \mid \mathbf{X})} \prod_{i=1}^{n} p(y_i \mid f_i) \tag{5}$$

and $p(y_i \mid f_i)$ can be calculated by equation (3) and $p(\boldsymbol{f} \mid \mathbf{X})$ is the GP prior over latent function. Since a GP is characterized by a mean function and a covariance function. Here, we use zero mean for symmetry reasons, and for covariance function we have selected linear covariance function which has been found to be effective in classification problems [24]. The normalization term in the denominator is the marginal likelihood given by

$$p(\mathbf{y} \mid \mathbf{X}) = \int p(\boldsymbol{f} \mid \mathbf{X}) \prod_{i=1}^{n} p(y_i \mid f_i) \tag{6}$$

where $\mathbf{y} = \{y_1, y_2, ...y_n\}$. The second term in the above equation is not Gaussian and this makes the posterior in equation (5) analytically intractable. Analytical approximations or Monte Carlo methods can be used. Two commonly used approximation methods are Laplace approximation and Expectation Propagation (EP). EP minimizes the local Kullback-Leibler (KL) divergence between the posterior and its approximation and has been found to be more accurate in predicting than Laplace approximation [18-19]. We use EP for approximation in our experiments.

Experiments and Results

Disease Detection

Thermal and stereo colour images from powdery mildew experiments on tomato plants were taken on 15 consecutive days. The results of image rectification and disparity estimation after rectification are shown in Figure 9. In this figure (a) and (b) show overlaid images from left (red) and right (cyan) cameras before and after rectification respectively. It is clear from (b) that the same features of plants lie on the same horizontal line. In the rectified image, pixels on the ground have zero disparity and as we move above the ground disparity increases. The result of disparity for this particular image pair is shown in Figure 9 (c). There is some noise from the background which can be removed. There are also some dark spots in the plant region in the disparity image, but these become part of disparity image because of occlusions. We are working on more sophisticated methods for disparity estimation for comparison in analysis.

Registration of thermal and colour images is a major part of this project and we are currently working on this problem. Preliminary results of our registration algorithm is shown in Figure 10 (c). In this figure the thermal image is overlaid on a registered colour image. There is still need for improvement and refinement of registration results as shown in Figure 11 (a). The

figure shows the result of registration and on the right a part of the image is shown after zooming in. It is clear that there are still some spaces in this registration result which are not yet aligned. We are currently working on refining our results so that the result of registration becomes more accurate. Another problem we are facing with registration is that the thermal images are not consistent in behaviour which is natural for these images as the disease progresses. Registration of these images become difficult because the shape of leaf becomes more irregular and it becomes difficult to distinguish the background from the plant. An example of such an image is shown in Figure 11 (b). The image shown is an enhanced version of the image, even in this enhanced image it is very difficult to distinguish between plant and the background. Another problem in this image is that some of the regions in the plant are at higher temperature from the ground and some of them are at a lower temperature from the ground. This makes it difficult to distinguish the regions belonging to plant and the background. We are working on the registration of these kinds of images, as soon as we get some good results for registration, we will be ready to do analysis on the collected data.

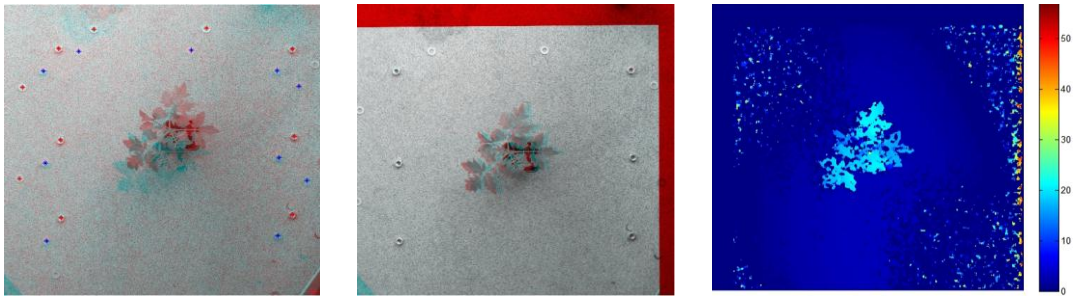

(a) (b) (c)

Figure 9: (a) shows images from left (red) and right (cyan) cameras before rectification. (b) shows images from left and right cameras after rectification. (c) shows the result of disparity estimation algorithm used in our experiments.

(a) (b) (c)

Figure 10: (a) & (b) show the colour and corresponding thermal image. (c) shows the registered thermal and color images with (inverted) thermal image overlaid on the colour image.

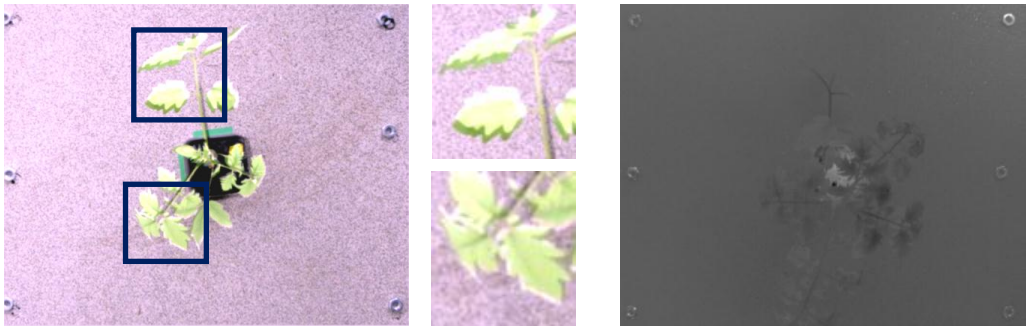

(a) (b)

Figure 11: (a) Result of registration on whole image is shown on left and on the right it shows zoomed image of registration result. (b) an enhanced version of a thermal image is shown from a diseased plant.

Stress Detection

A total of 108 images of a spinach canopy were obtained, 54 images were taken from well-watered plants (treatment A) and 54 images were from a drought canopy (treatment B). After pre-processing, six different features (first six from

Table **1**) were obtained from each image. We use SVM and GPCs to classify the test images into drought and well-watered. For SVM we used linear kernel and for GPC we choose zero mean and a linear covariance function. As discussed before, SVM gives discrete classification results and we get each image classified as treatment A or Treatment B image, whereas, GPCs give probability of each image to belong to treatment B vs the values of soil moisture as shown in Figure 12. It is clear from Figure 12 that classification results shown by our classifier are in agreement to with the manually calculated soil moisture values. Based on the probabilities given by GPC, we can efficiently classify the image as an image from treatment A or treatment B canopy.

Since we are using two different types of classifiers we noticed disagreement in the results of both classifiers in some cases. We can use this disagreement to further refine our classification results. We combine information from both the classification methods to reduce the error from classification. If an image is classified by SVM as treatment A, we check its probability of belonging to treatment B as given by GPC. If the probability is higher than 80% then we classify this image as treatment B. On the other hand if an image is classified as treatment B and its probability according to GPC is less than 20%, we classify this image as image from treatment A.

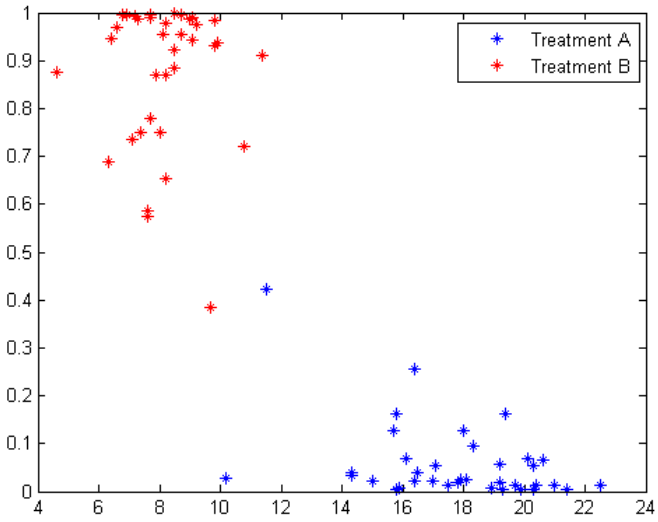

Figure 12: Probability of belonging to treatment B vs Soil moisture values (correlation value = - 0.89, High moisture means less probability of stress) (%Volume) as given by our classifier. Classification accuracy for this particular set of training and testing data set was about 98.62%.

We ran 200 iterations to test the accuracy of our classifiers for different pairs of the training and testing data sets. In each iteration, we randomly picked 36 images (18 from each treatment) for training purpose and tested our algorithm on the rest of the 72 images. The results for different classifiers are given in

Table 2. GPC shows better results than SVM classifier; however it can be seen that if we combine information from both the classifiers, we get better results in terms of sensitivity, specificity, positive predictive value (PPV) and accuracy. We obtained an average accuracy of 96.27% by using SVM, 96.68% by using GPC and a slightly higher 97.12% when we combine the information from both the classifiers. We have compared our results with colour only and temperature only features and we have found that combining information from both temperature and colour data increases the accuracy of classification. We have found that including mean and standard deviation without combining them with colour information deteriorate the performance of our results, so we remove mean (μ_T) and standard deviation (σ_T) from our set of features.

Table 2: Comparison of average classification results of different classifiers using our algorithm.

Feature(s) selected	Classifier	Sensitivity (%)	Specificity (%)	PPV (%)	Accuracy (%)	σ_{accuracy}
Colour only (μ_a, μ_b)	SVM	67.28	70.29	70.98	67.74	3.36
	GPC	80.68	52.96	21.68	56.87	3.55
	Both Classifiers	67.32	70.42	71.11	67.80	3.40
Thermal only (μ_T, σ_T)	SVM	93.35	91.28	90.89	92.14	1.92
	GPC	93.06	80.30	76.67	85.42	2.29
	Both Classifiers	93.35	91.28	90.88	92.14	1.92
Features (1-8) Table 1.	SVM	95.52	96.39	96.30	95.85	1.97
	GPC	96.38	97.39	97.30	96.79	1.56
	Both Classifiers	96.62	96.93	96.84	96.70	1.60
Features (1-6) Table 1.	SVM	95.86	96.86	96.80	96.27	1.58
	GPC	96.53	96.99	96.90	96.68	2.00
	Both Classifiers	96.97	97.38	97.31	97.12	1.52

In our experiments, we found that scaling with luminance intensity (μ_{LT}) plays a major role in classification. We removed luminance intensity scaling feature (p-value = 0.154) from our set of features, we found that accuracy of the classifiers falls as given in Table 3. In case of GPC classification accuracy falls up to 7%. This shows that not only selection of good features is very important when we classify the data from thermal images for stress analysis but also information from corresponding colour image is very useful. A video demonstration of the software developed for this purpose can be viewed at

http://www.youtube.com/watch?v=kNwChVGGZIE. A snapshot of the software is given in Figure 13.

Table 3: Comparison of average classification results of different classifiers without using light intensity scaling feature (μ_{LT}). [OPTIONAL]

	Sensitivity (%)	Specificity (%)	PPV (%)	Accuracy (%)	$\sigma_{accuracy}$
SVM	94.98	95.01	94.83	94.84	2.01
GPC	88.21	91.84	92.05	89.70	2.61
Both Classifiers	95.28	95.27	95.08	95.12	1.89

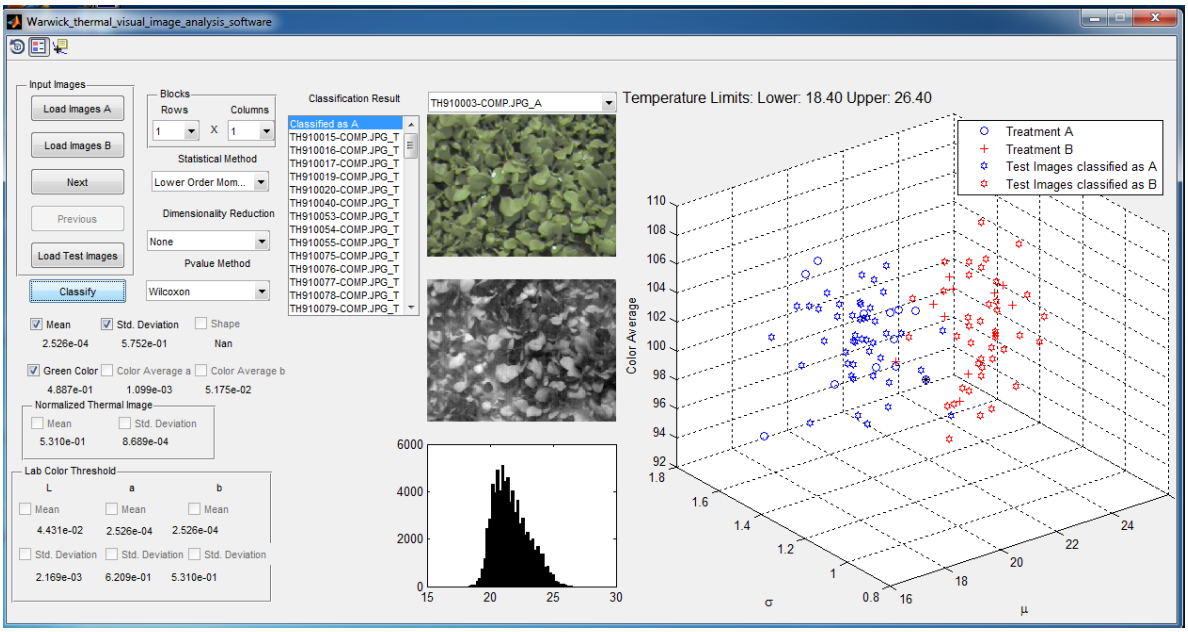

Figure 13: Snapshot of the software developed for analysis of drought plants

Conclusions and Future Work

In this report, we have presented the algorithms, experiments and results obtained during the last year for combined thermal and colour image analysis of plants for disease and stress detection. On the disease detection part of the project we have collected data from a powdery mildew experiment being performed on tomato plants. Thermal and colour image data was collected every day for about two weeks along with manual measurements of temperature values for a couple of days. We have developed and tested algorithms for image rectification, disparity estimation and registration of thermal and colour images. We are satisfied with the results of image rectification but need to develop more sophisticated algorithms for disparity estimation and registration of thermal and colour images.

Registration of thermal and colour images is currently the main focus of our work, as good registration is necessary for combined analysis of thermal and colour data. On the stress analysis of the spinach canopy we have achieved some good results and we are working closely with collaborators at University of Southampton for publication and analysis of more data if available. The future work plan is as follows:

1) Refine registration algorithm (disease data) and enhance its capability to register noisy thermal images.
2) Following 1), use various statistical approaches for analysis of the disease images and compare results using different depth estimation algorithms. Analysis of images from diseased plants can be extended and compared with results obtained from stress experiment to see if a crop under stress can be distinguished from a crop under attack of disease.
3) Capture more data from the industry so that we can modify and enhance our algorithms for practical use. We have applied for acquisition of EPSRC Cedip Titanium thermal imaging camera, which we hope to get in August-September 2013. Once we get the confirmation from EPSRC we will liaise with industry to make an arrangement for imaging setup. Currently, we plan to do imaging at Bordon Hill nurseries and Double H nurseries.

References

[1] H. G. Jones, “Use of infrared thermometry for estimation of stomatal conductance as a possible aid to irrigation scheduling,” *Agricultural and Forest Meteorology*, vol. 95, no. 3, pp. 139–149, 1999.

[2] H. G. Jones, M. Stoll, T. Santos, C. de Sousa, M. M. Chaves, and O. M. Grant, “Use of infrared thermography for monitoring stomatal closure in the field: application to grapevine,” *Journal of Experimental Botany*, vol. 53, no. 378, pp. 2249–2260, 2002.

[3] H. G. Jones, *Plants and Microclimate: a quantitative approach to environmental plant physiology.*, 2nd ed. Cambridge: Cambridge University Press, 1992.

[4] L. Chaerle, W. Van Caeneghem, and E. Messens, “Presymptomatic visualization of plant-virus interactions by thermography,” *Nature*, vol. 17, no. 8, pp. 813–6, Aug. 1999.

[5] L. Chaerle, I. Leinonen, H. G. Jones, and D. Van Der Straeten, “Monitoring and screening plant populations with combined thermal and chlorophyll fluorescence imaging.,” *Journal of Experimental Botany*, vol. 58, no. 4, pp. 773–84, Jan. 2007.

[6] E.-C. Oerke, U. Steiner, H.-W. Dehne, and M. Lindenthal, “Thermal imaging of cucumber leaves affected by downy mildew and environmental conditions.,” *Journal of Experimental Botany*, vol. 57, no. 9, pp. 2121–32, Jan. 2006.

[7] E. Trucco and A. Verri, *Introductory Techniques for 3-D Computer Vision*. Prentice Hall, 1998.

[8] R. D. Jackson, S. B. Idso, R. J. Reginato, and P. J. Pinter, “Canopy Temperature as a Crop Water-Stress Indicator,” *Water Resources Research*, vol. 17, no. 4, pp. 1133–1138, 1981.

[9] S. B. Idso, R. D. Jackson, P. J. Pinter Jr, R. J. Reginato, and J. L. Hatfield, “Normalizing the stress-degree-day parameter for environmental variability,” *Agricultural Meteorology*, vol. 24, no. 1, pp. 45–55, 1981.
[10] V. Alchanatis, Y. Cohen, S. Cohen, M. Moller, M. Sprinstin, M. Meron, J. Tsipris, Y. Saranga, and E. Sela, “Evaluation of different approaches for estimating and mapping crop water status in cotton with thermal imaging,” *Precision Agriculture*, vol. 11, no. 1, pp. 27–41, 2009.
[11] S. Reinert, R. Bögelein, and F. M. Thomas, “Use of thermal imaging to determine leaf conductance along a canopy gradient in European beech (Fagus sylvatica).,” *Tree physiology*, vol. 32, no. 3, pp. 294–302, 2012.
[12] R. Hartley and A. Zisserman, *Multiple View Geometry in Computer Vision*. Cambridge University Press, 2003.
[13] A. Goshtasby, “Piecewise linear mapping functions for image registration,” vol. 19, no. 6, pp. 459–466, 1986.
[14] R. M. Pherwani, *Determine object location using a stereo disparity vision system*. Cornell University, Jan., 1988.
[15] K. Konolige, “Small vision systems: Hardware and implementation,” *ROBOTICS RESEARCH-INTERNATIONAL*, 1998.
[16] L. Eikvil, “Optical Character Recognition,” Oslo, 1993.
[17] P. Perona and J. Malik, “Scale-space and edge detection using anisotropic diffusion,” *IEEE Transactions on Pattern Analysis and Machine Intelligence*, vol. 12, no. 7, pp. 629–639, Jul. 1990.
[18] O. M. Grant, M. M. Chaves, and H. G. Jones, “Optimizing thermal imaging as a technique for detecting stomatal closure induced by drought stress under greenhouse conditions,” *Physiologia Plantarum*, vol. 127, no. 3, pp. 507–518, 2006.
[19] O. M. Grant, L. Tronina, H. G. Jones, and M. M. Chaves, “Exploring thermal imaging variables for the detection of stress responses in grapevine under different irrigation regimes.,” *Journal of Experimental Botany*, vol. 58, no. 4, pp. 815–25, 2007.
[20] M. Stoll and H. Jones, “Thermal imaging as a viable tool for monitoring plant stress,” *Journal International des Sciences de la Vigne et du Vin*, vol. 41, no. 2, pp. 77–84, 2007.
[21] M. Möller, V. Alchanatis, Y. Cohen, M. Meron, J. Tsipris, A. Naor, V. Ostrovsky, M. Sprintsin, and S. Cohen, “Use of thermal and visible imagery for estimating crop water status of irrigated grapevine.,” *Journal of experimental botany*, vol. 58, no. 4, pp. 827–38, 2007.
[22] I. Leinonen and H. G. Jones, “Combining thermal and visible imagery for estimating canopy temperature and identifying plant stress.,” *Journal of Experimental Botany*, vol. 55, no. 401, pp. 1423–31, 2004.
[23] C. Cortes and V. Vapnik, “Support-vector networks,” *Machine Learning*, vol. 20, no. 3, pp. 273–297, 1995.
[24] C. E. Rasmussen and C. K. Williams, *Gaussian processes for machine learning*. Cambridge: MIT Press, 2006.
[25] C. Rasmussen, “Gaussian processes in machine learning,” *Advanced Lectures on Machine Learning*, pp. 63–71, 2004.
[26] G. Haranadh and C. C. Sekhar, “Hyperparameters of Gaussian process as features for trajectory classification,” *Neural Networks (IEEE World Congress on Computational Intelligence), IEEE International Joint Conference on*, no. 3, pp. 2195–2199, 2008.
[27] Y. Bazi and F. Melgani, “Gaussian process approach to remote sensing image classification,” *Geoscience and Remote Sensing, IEEE Transactions on*, vol. 48, no. 1, pp. 186–197, 2010.
[28] M. Ebden, “Gaussian Processes for Regression : A Quick Introduction,” no. August, 2008.

[29] M. Kuss and C. Rasmussen, “Assessing approximate inference for binary Gaussian process classification,” *The Journal of Machine Learning Research*, vol. 6, pp. 1679–1704, 2005.
[30] T. Minka, “Expectation propagation for approximate Bayesian inference,” *Proceedings of the Seventeenth conference on Uncertainty in artificial intelligence.*, 2001.

